NASA CONTRACTOR REPORT

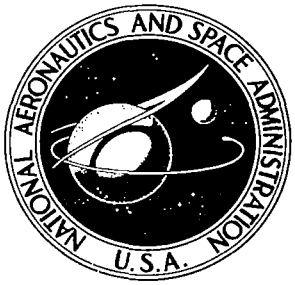

NASA CR-2649

STOCHASTIC SEA STATE FOR SRB STUDIES

M. Perlmutter and M. E. Graves

Prepared by
NORTHROP SERVICES, INC.
Huntsville, Ala.
for George C. Marshall Space Flight Center

NATIONAL AERONAUTICS AND SPACE ADMINISTRATION • WASHINGTON, D. C. • FEBRUARY 1976

TECHNICAL REPORT STANDARD TITLE PAGE

1. REPORT NO. NASA CR-2649	2. GOVERNMENT ACCESSION NO.	3. RECIPIENT'S CATALOG NO.
4. TITLE AND SUBTITLE Stochastic Sea State for SRB Studies		5. REPORT DATE February 1976 6. PERFORMING ORGANIZATION CODE M166
7. AUTHOR(S) M. Perlmutter and M. E. Graves		8. PERFORMING ORGANIZATION REPORT #
9. PERFORMING ORGANIZATION NAME AND ADDRESS Northrop Services, Inc. Huntsville, Alabama		10. WORK UNIT NO. 11. CONTRACT OR GRANT NO. NAS8-21810
12. SPONSORING AGENCY NAME AND ADDRESS NASA Washington, D. C. 20546		13. TYPE OF REPORT & PERIOD COVERED Contractor Report 14. SPONSORING AGENCY CODE

15. SUPPLEMENTARY NOTES

Prepared under the technical monitorship of the Aerospace Environment Division, Space Sciences Laboratory, NASA-Marshall Space Flight Center.

16. ABSTRACT

Ocean surface characteristics at two locations are studied for a Space Shuttle solid rocket booster ocean impact and recovery analysis. Probability distributions of wave heights, wave slopes, wave velocities, ocean currents, and 1-kilometer altitude winds are formulated. Procedures for generating ocean wave simulations are also described.

17. KEY WORDS Ocean Waves Wind Waves Stochastic Processes Sea State	18. DISTRIBUTION STATEMENT Category 48

19. SECURITY CLASSIF. (of this report)	20. SECURITY CLASSIF. (of this page)	21. NO. OF PAGES	22. PRICE
UNCLASSIFIED	UNCLASSIFIED	46	$3.75

For sale by the National Technical Information Service, Springfield, Virginia 22161

FOREWORD

This report presents the results of work done by Northrop Services, Inc., Huntsville, Alabama, for the National Aeronautics and Space Administration, George C. Marshall Space Flight Center, under Contract NAS8-21810. The work was performed for the Science and Engineering Directorate in response to the requirements of Appendix A, Schedule Order Number A02Z (A-13) Paragraph 1, Tasks 1.1 and 1.4.

Dr. George H. Fichtl was the Technical Coordinator for this task, and the authors are grateful for his guidance and fruitful discussions during the work.

TABLE OF CONTENTS

LIST OF ILLUSTRATIONS

LIST OF TABLES

Section 1

INTRODUCTION

The Solid Rocket Booster (SRB) of the Space Shuttle is expected to descend and impact into the ocean shortly after launch. Current plans call for the recovery of the SRB's from the ocean. In order to estimate the probable loss or damage to the SRB's in the recovery process, the following information is needed:

- Ocean current and direction distribution
- One-kilometer altitude winds
- Wave height distribution
- Wave slope distribution
- Vertical wave velocity distribution
- Horizontal wave velocity distribution.

This information is required at the two locations presently being considered for ocean entry and recovery operations. These locations are the Cape Kennedy, Florida, Atlantic coastal waters bounded by 24 to 30 degrees north latitude, 75 to 80 degrees west longitude; and the Vandenberg AFB, California, coastal waters, bounded by 31 to 33 degrees north latitude, 120 to 122 degrees west longitude.

To improve our estimate of losses of and damage to the SRB, a simulation of the behavior of the ocean waves would be valuable. Such a simulation is important in order to assess the interaction of the SRB with the ocean and to calculate the stress loadings caused by the waves. In this study, only methods for simulating long-crested waves are developed. The simulation of more general cases remains for future work.

Extensive work has been done in the study of ocean waves (References 7 through 11), but substantially less work has been done in ocean simulations. No previous work, as far as we know, has been carried out using the control system model approach to ocean wave simulation.

This report also discusses and presents in tabular form the statistical distribution and sampling procedures to be used in simulation studies for the ocean currents (Section II) and for the 1-kilometer winds (Section III). In Section IV the long-crested wave model is developed and discussed, the Pierson-Moskowitz spectrum is given, and the equations are normalized. In Section V, two simulation procedures are developed and described. The statistical distributions of the wave height, wave slope, and surface velocity components, as well as velocities below the surface, are given in Section VI.

Section II

OCEAN CURRENTS

2.1 GENERAL

To simulate an ocean current for a study of the Solid Rocket Booster (SRB) splashdown and recovery, the joint probability distribution $f_{\theta,w}$ of the current speed w and direction θ are required. The term $f_{\theta,w}$ is given by the product of the marginal distribution of w, f_w, and the conditional distribution of θ given w, $f_{\theta|w}$.

The simulation of ocean currents requires the sampling of values of w and θ from $f_{\theta|w} f_w$. The sampling procedure first samples w from the marginal distribution, f_w; then this value is used in the conditional distribution $f_{\theta|w}$ to sample the value of θ.

Computer subroutines are available to generate uniformly distributed pseudo-random numbers, R_w, between 0 and 1. A common method of random sampling from a distribution f(w) is to first randomly obtain R_w, then use a transformation to obtain the sampled value of w. This relationship is given by (see Reference 1)

$$R_w = F_w = \int_0^w f(w')\, dw' \qquad (2.1)$$

where F_w is the cumulative distribution of the ocean current speed.

Thus, the procedure is to have the computer generate a value of R_w, then solve Equation 2.1 for w. This is accomplished by using an interpolation scheme as follows. At discrete values of F_w, [F_w = 0, .1, .2, ..., 1.0], the corresponding values of w are obtained. These values are inputted into a spline curve-fitting routine along with the values of the initial and final derivatives,

$$\left.\frac{dw}{dF_w}\right|_{F_w=0} \text{ and } \left.\frac{dw}{dF_w}\right|_{F_w=1} .$$

The routine fits cubic curves between adjacent input values, and it requires continuous values of the function and its first derivative at each point. Then for each sampled value of R_w which is set equal to F(w), the appropriate sampled value of w is obtained by interpolation.

The spline-fitting using the input data is available on the UNIVAC 1108 as a subroutine SPLN1 (Reference 2). To obtain interpolated values of w for given values of R_w, use is made of the subroutine SPLN2. This procedure will be illustrated in the following subsections.

2.2 OCEAN CURRENT SPEED

The cumulative distribution of the ocean current speed F_w needed for the random sampling is given in Table 2-1 along with the required derivatives $\frac{dw}{dF_w}$ at F_w=0 and at F_w=1. These results were obtained from Reference 3.

The general terms, "summer" and "winter" in the table refer to the months, May through October and November through April, respectively. The three oceanic areas are areas 22 and 26, which are off the Atlantic coast near Kennedy Space Center (KSC), and an area which is off the Pacific coast near Vandenberg Air Force Base (VAFB). These areas are shown on Figure 2-1.

In the simulation procedure used to sample randomly from the distribution f_w, the data F_w and the corresponding values of w given in Table 2-1 are first inputted into the subprogram, SPLN1. Then a random number R_w is generated. Setting R_w equal to F_w and using the subprogram SPLN2, the interpolated value of w is obtained for use in the simulation.

On Figure 2-2, the values entered into the spline routine are shown, as well as the interpolated values found by the spline routine for an illustrative case.

2.3 CONDITIONAL OCEAN CURRENT DIRECTION

Once the ocean current speed w has been sampled, the ocean current direction θ is then randomly sampled for each given value of w. Similar to Equation (2.1), Equation (2.2) can be written as

Table 2-1. MARGINAL CUMULATIVE DISTRIBUTION OF OCEAN CURRENT SPEED (KNOTS) FOR USE IN SPLINE CURVE INTERPOLATION

LOCATION	CUMULATIVE FREQUENCY (F_w)												
	a*	0	.10	.20	.30	.40	.50	.60	.70	.80	.90	1.00	b**
KSC													
AREA 22:													
SUMMER	0.0	0.0	0.0	0.1	0.2	0.4	0.5	0.7	0.8	1.1	1.4	6.5	30.
WINTER	0.0	0.0	0.1	0.2	0.3	0.4	0.5	0.7	0.9	1.1	1.5	6.5	30.
AREA 26:													
SUMMER	10.0	0.0	0.3	1.2	1.7	2.1	2.5	2.8	3.1	3.4	3.8	6.5	15.
WINTER	10.0	0.0	0.5	1.0	1.5	1.9	2.4	2.6	2.9	3.2	3.6	6.9	15.
VAFB													
SUMMER	0.0	0.0	0.0	0.0	0.1	0.1	0.2	0.3	0.4	0.7	0.9	3.5	30.
WINTER	0.0	0.0	0.0	0.0	0.1	0.1	0.2	0.2	0.3	0.4	0.7	3.0	30.

* $a = \frac{dw}{dF_w} \Big|_{(F_w = 0)}$

** $b = \frac{dw}{dF_w} \Big|_{(F_w = 1)}$

OCEAN CURRENT SPEED AND DIRECTION DATA WERE PROCESSED FOR THREE DESIGNATED AREAS, NAMELY AN AREA ALONG THE LOWER CALIFORNIA COAST AND AREAS 22 AND 26 OFF THE FLORIDA COAST. THE CALIFORNIA AREA VARIES SEASONALLY FROM THE BOUNDARIES SHOWN HERE, WHEREAS AREAS 22 AND 26 ARE UNCHANGING.

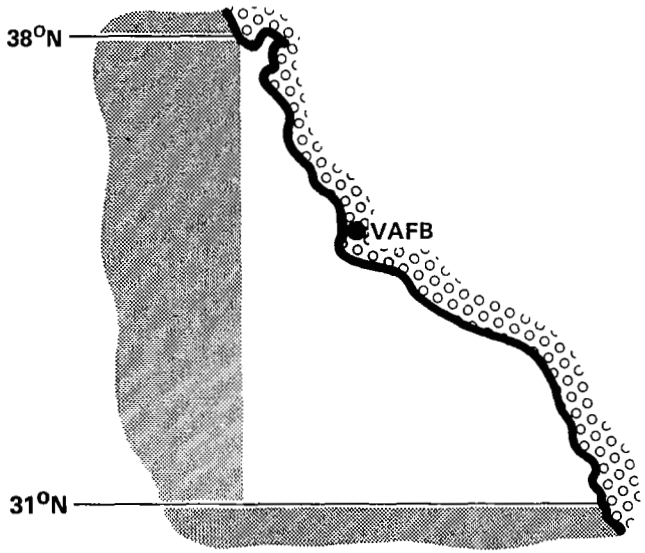

LOCATION OF AREA ALONG THE LOWER CALIFORNIA COAST IN THE VICINITY OF VANDENBERG AFB (VAFB)

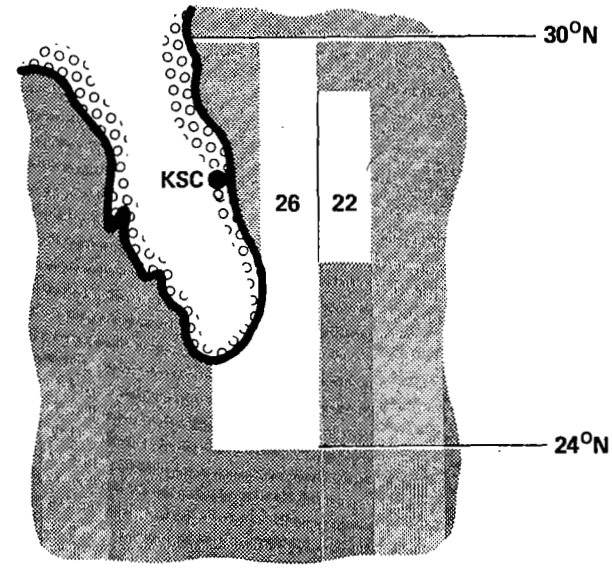

LOCATION OF AREAS 22 AND 26 OFF THE FLORIDA COAST IN THE VICINITY OF KENNEDY SPACE CENTER (KSC)

Figure 2-1. LOCATION OF SRB IMPACT ZONES

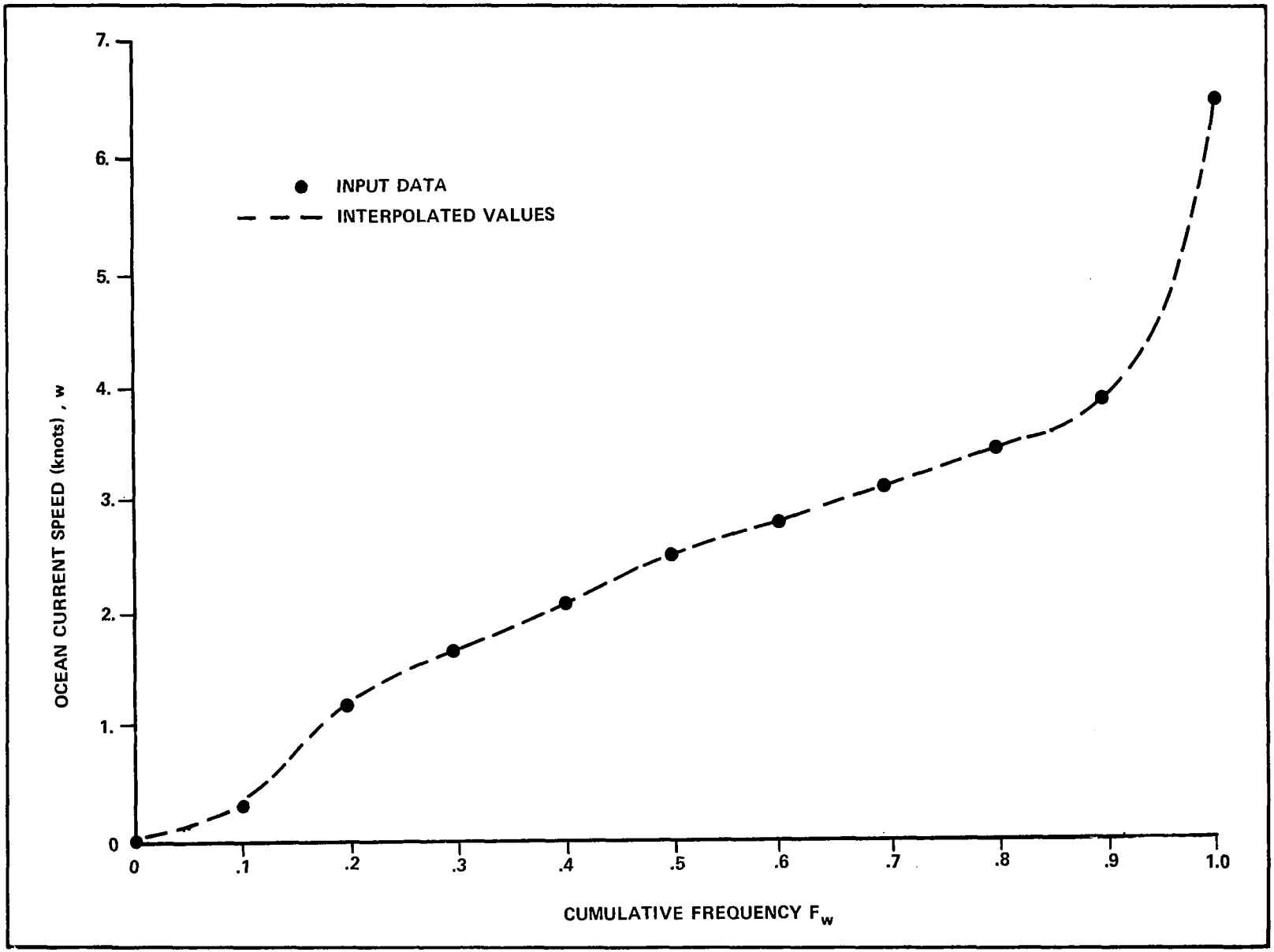

Figure 2-2. MARGINAL CUMULATIVE FREQUENCY, FREQUENCY, F_w, OF OCEAN CURRENT SPEED (KNOTS) KSC AREA 26 SUMMER

$$R_\theta = F_{\theta|w} = \int_0^\theta f(\theta'|w)\, d\theta' \qquad (2.2)$$

where $F_{\theta|w}$ is the conditional, cumulative distribution of θ for a given value of w. Thus, the same procedure is followed for θ as for w; namely, another random number, R_θ, is generated and set equal to $F_{\theta|w}$ to obtain the value of θ, using the spline curve interpolation of the appropriate cumulative distribution.

The conditional, cumulative distribution for θ and the derivatives at the extrema of F_w are given in Table 2-2 for use in the spline interpolation program. These are given for the same geographic regions and time periods as in subsection 2.2. "Summer" and "winter" have the same measurable ranges as in Table 2-1.

In Figure 2-3, an illustrative set of data points to be inputted into the spline routine is shown along with the interpolated values obtained from the spline routine.

By generating two random numbers, R_w and R_θ, a selection can be made from the appropriate statistical distribution sample values of ocean current speed w and ocean current direction θ for use in SRB ocean studies. A large number of sample values of w and θ will satisfy the appropriate distribution of $f_{\theta,w}$.

Table 2-2. CONDITIONAL CUMULATIVE DISTRIBUTION OF OCEAN CURRENT DIRECTION (DEGREES), GIVEN OCEAN CURRENT SPEED (KNOTS), FOR SPLINE CURVE INTERPOLATION

LOCATION	CUMULATIVE FREQUENCY												
	a*	0	.10	.20	.30	.40	.50	.60	.70	.80	.90	1.00	b**
KSC													
AREA 22: SUMMER													
$0 \leq w < 1.0$	0	0	0	12	45	135	164	184	197	213	251	360	9.0
$1.0 \leq w$	0	0	0	0	16	39	151	176	186	192	202	360	5.0
WINTER													
$0 \leq w < 1.0$	0	0	0	24	86	148	173	197	202	217	253	360	9.0
$1.0 \leq w$	0	0	0	11	123	165	184	202	206	218	251	360	9.0
AREA 26: SUMMER													
$0 \leq w < 1.0$	0	0	0	0	0	0	6	19	31	97	140	360	6.0
$1.0 \leq w$	0	0	0	0	0	0	0	3	12	22	37	360	14.0
WINTER													
$0 \leq w < 1.0$	0	0	0	0	0	0	0	0	15	32	72	360	11.0
$1.0 \leq w$	0	0	0	0	0	0	0	5	16	28	45	360	15.0
VAFB													
AREA 23: SUMMER													
$0 \leq w < 0.9$	0	0	0	63	100	125	146	164	190	232	272	360	8.0
$0.9 \leq w$	0	0	0	62	84	103	122	141	164	273	285	360	6.0
WINTER													
$0 \leq w < 0.9$	0	0	19	80	103	118	133	148	165	190	246	360	10.0
$0.9 \leq w$	0	40	75	92	103	111	119	127	136	143	154	360	6.0

* $a = \left.\frac{d\theta}{dF_{\theta|w}}\right|_{F_{\theta|w} = 0}$

** $b = \left.\frac{d\theta}{dF_{\theta|w}}\right|_{F_{\theta|w} = 1} \times 0.01$

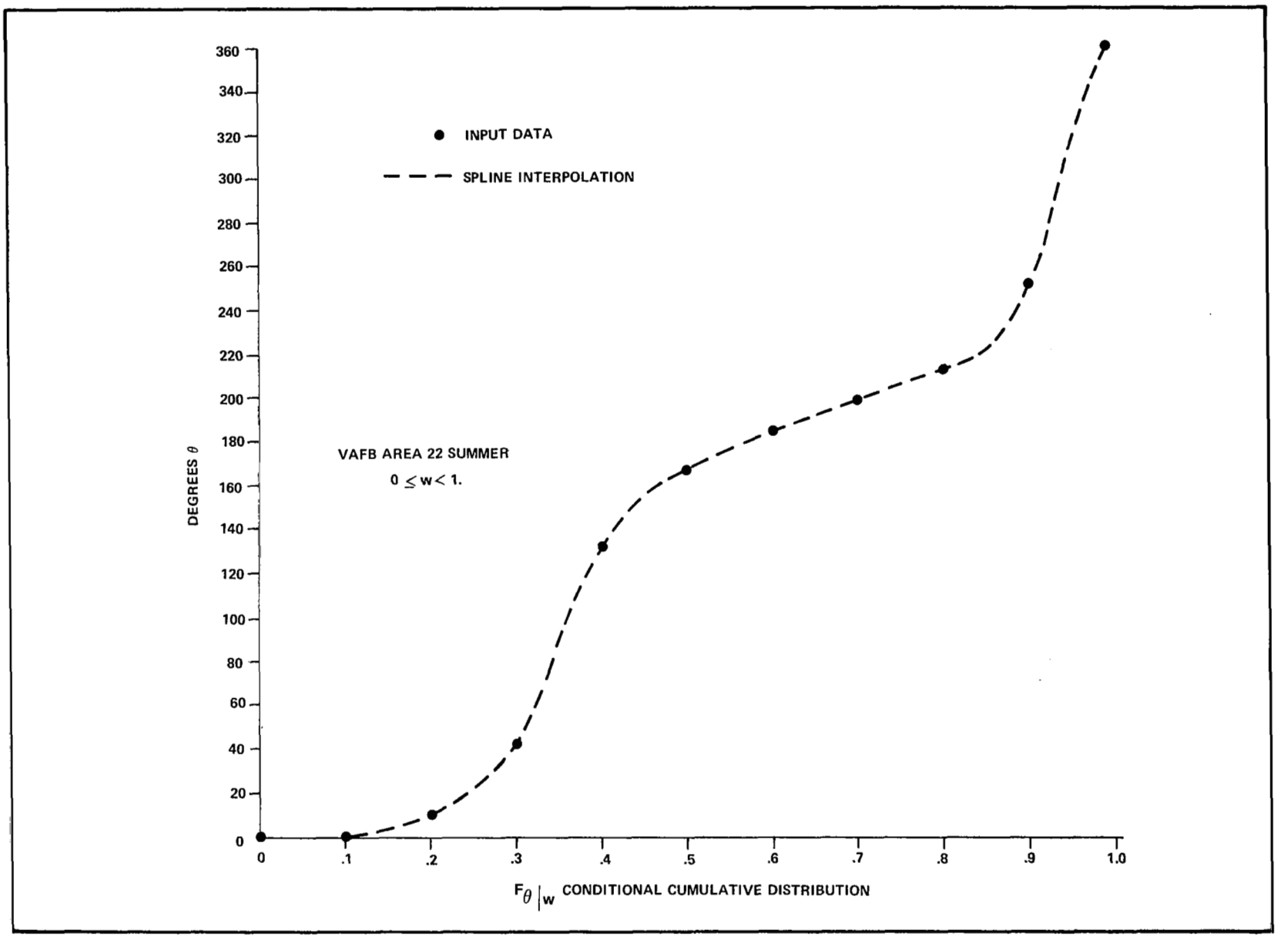

Figure 2-3. CONDITIONAL CUMULATIVE FREQUENCY ($F_{\theta|w}$), OF OCEAN CURRENT DIRECTION (DEGREES), VAFB AREA 22 SUMMER

Section III

ONE-KILOMETER WINDS

3.1 GENERAL

For the purpose of simulating ocean conditions, knowledge of the joint distribution of wind direction and wind velocity at the 1-kilometer altitude is also required. As in subsection 2.1, the joint distribution of the wind speed v and the wind direction ϕ are written as a product of the marginal distribution of v, f_v, times the conditional distribution of ϕ for a given v, $f_{\phi|v}$. As before

$$f_{\phi,v} = f_{\phi|v} f_v \quad .$$

3.2 ONE-KILOMETER WIND SPEED

The cumulative distribution of v, F_v, is represented in tabular and graphical form in Table 3-1 and Figure 3-1. These values were obtained from Reference 4. Table 3-1 gives the marginal, cumulative distribution values, F_v, for the corresponding values of v as well as values of the derivatives $\left(\frac{dv}{dF_v}\right)$ at $F_v = 0$ and at $F_v = 1$, for use in the spline interpolation. To sample v from f_v we generate R_v from a uniform distribution, set it equal to F_v, then find v by interpolation.

3.3 ONE-KILOMETER WIND DIRECTION

Analogous to subsection 2.3, once the wind velocity has been sampled, the wind direction is randomly sampled. This can be done through the conditional, cumulative distribution $F_{\phi|v}$ of the wind direction ϕ for a given value of wind velocity v. The values needed for implementing the spline fit are given in Table 3-2 for the KSC geographical area and in Table 3-3 for the VAFB geographical area. Examples of the cumulative distribution of data points used in the spline fit and the interpolated results are presented on Figure 3-2. To sample the wind direction ϕ we generate a random number R_ϕ from a uniform distribution, set it equal to $F_{\phi|v}$ where the v has been obtained previously, and interpolate the random value ϕ.

The discussion in subsection 2.3 on sampling ocean currents is applicable here to the sampling of winds.

Table 3-1. MARGINAL CUMULATIVE DISTRIBUTION OF SCALAR WIND SPEED AT 1 KM (m/sec)

LOCATION	CUMULATIVE FREQUENCY (F_V)												
	a*	0	.10	.20	.30	.40	.50	.60	.70	.80	.90	1.00	b**
KSC													
JAN	0.4	0	2.7	4.3	5.6	6.8	7.4	9.1	10.4	12.0	15.0	26.9	5.7
FEB	0.3	0	2.7	4.2	5.5	6.5	7.5	9.0	10.9	13.1	16.3	28.0	3.5
MAR	0.0	0	1.5	2.2	2.8	3.3	3.6	4.5	5.5	6.7	9.5	22.7	3.0
APR	0.2	0	2.2	3.6	4.7	5.7	6.6	7.5	8.6	9.8	13.0	24.0	3.4
MAY	0.1	0	1.7	2.6	3.5	4.3	5.0	5.9	7.0	8.1	9.8	18.6	4.0
JUN	0.1	0	1.6	2.4	3.1	3.8	4.5	5.2	6.1	7.1	9.3	25.0	12.0
JUL	0.1	0	1.6	2.4	3.1	3.8	4.5	5.2	6.1	7.1	9.2	24.9	12.0
AUG	0.0	0	1.3	2.2	3.0	3.7	4.3	5.0	5.8	6.7	8.2	20.9	9.0
SEP	0.1	0	1.5	2.5	3.5	4.4	5.4	6.5	7.6	9.0	11.7	32.5	11.0
OCT	0.1	0	2.1	3.5	4.4	5.2	6.1	7.1	8.3	9.7	11.8	19.9	3.5
NOV	0.3	0	2.6	3.8	4.8	5.6	6.5	7.5	8.6	10.0	12.2	23.5	4.0
DEC	0.4	0	2.7	4.0	5.2	6.2	7.1	8.2	9.4	10.7	12.9	22.9	4.0
VAFB													
JAN	0.1	0	1.4	2.6	3.7	4.7	5.6	7.1	8.5	10.2	12.7	23.7	5.0
FEB	0.1	0	1.8	3.1	4.4	5.6	6.5	7.7	9.0	10.7	13.1	20.4	8.0
MAR	0.2	0	2.0	3.1	4.3	5.4	6.5	7.7	8.9	10.1	12.2	18.7	8.0
APR	0.3	0	2.5	3.7	4.8	5.7	6.5	7.4	8.4	9.5	11.2	21.4	12.0
MAY	0.1	0	1.5	2.6	3.5	4.3	5.0	6.1	7.3	8.6	10.3	17.3	8.0
JUN	0.1	0	1.5	2.4	3.4	4.0	4.6	5.6	6.7	7.8	9.5	19.4	12.0
JUL	0.1	0	1.1	1.9	2.5	3.0	3.5	4.2	4.9	5.8	7.3	14.3	8.0
AUG	0.1	0	1.2	1.7	2.0	2.3	2.6	3.7	4.9	6.2	8.2	13.7	6.0
SEP	0.1	0	1.0	1.7	2.1	2.4	2.7	3.7	4.8	6.3	8.2	13.4	6.0
OCT	0.1	0	1.0	1.8	2.8	3.6	4.3	5.3	6.3	7.7	9.8	22.3	14.0
NOV	0.1	0	1.5	2.5	3.5	4.3	5.2	6.6	8.0	9.7	11.9	24.4	13.0
DEC	0.2	0	1.8	3.2	4.4	5.4	6.5	7.8	9.2	10.8	13.2	20.3	8.0

* $a = \left.\frac{dv}{dF_v}\right|_{F=0}$

** $b = \left.\frac{dv}{dF_v}\right|_{F=1}$

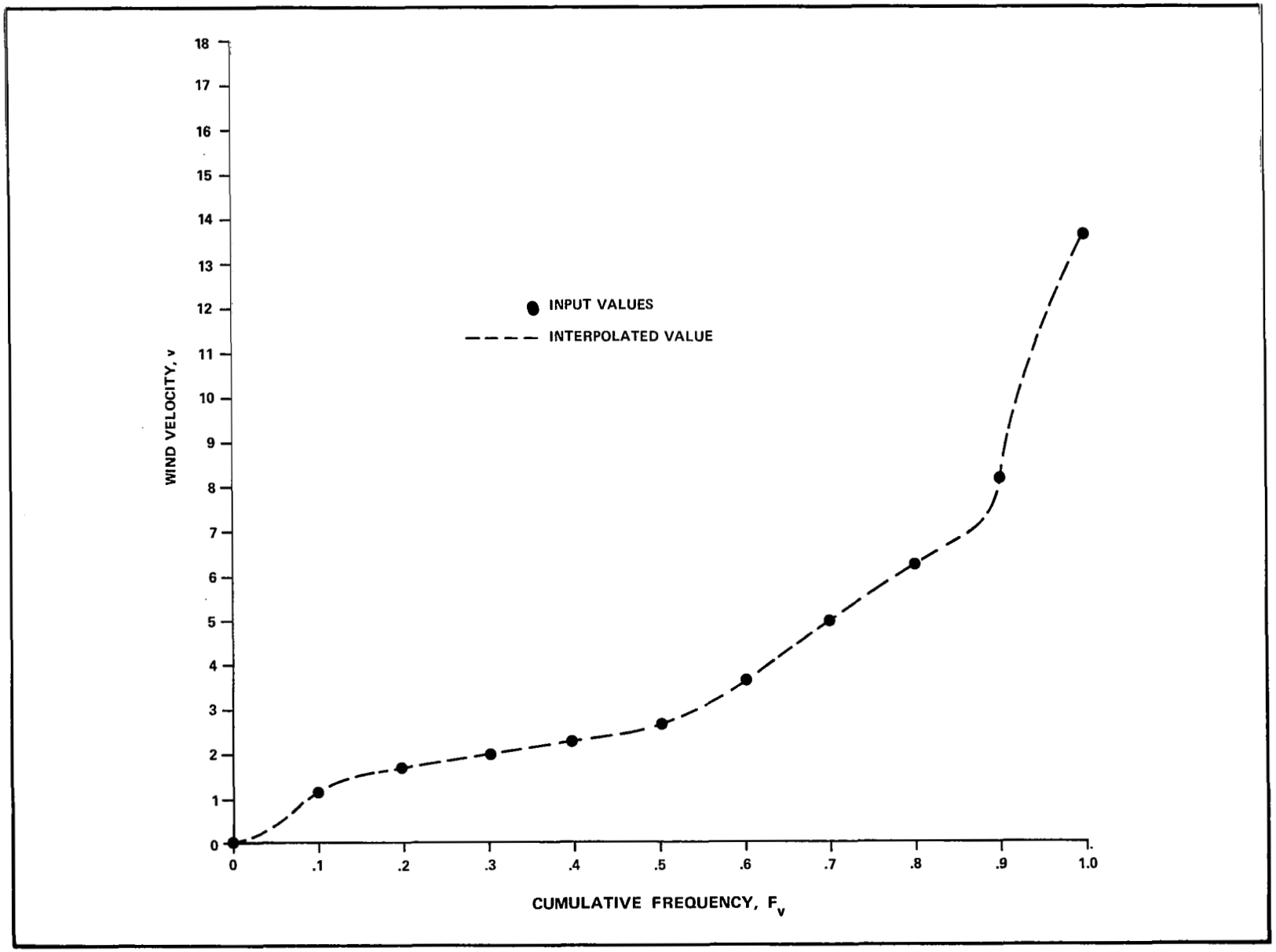

Figure 3-1. MARGINAL CUMULATIVE FREQUENCY (F_v) OF WIND SPEED (v) (m/sec) AT 1 KM ALTITUDE, VAFB, AUGUST

Table 3-2. CONDITIONAL CUMULATIVE DISTRIBUTION OF WIND DIRECTION (DEGREES), GIVEN WIND SPEED AT 1 KM (m/sec), AT KSC GEOGRAPHICAL AREA, FOR SPLINE CURVE INTERPOLATION

KSC	m/sec	CUMULATIVE FREQUENCY												
		a*	0	.10	.20	.30	.40	.50	.60	.70	.80	.90	1.00	b**
JAN	0<v≤5	2	0	49	113	147	166	194	225	252	279	311	360	7
	5<v≤10	6	0	61	92	127	157	195	240	264	290	311	360	8
	10<v≤15	9	0	79	171	197	218	232	250	267	289	311	360	9
	15<v≤20	34	0	189	210	236	245	254	263	275	286	300	360	5
	20<v≤25	31	0	173	188	197	205	210	222	237	256	275	360	12
	25<v	29	0	170	185	190	195	203	209	236	255	275	360	12
FEB	0<v≤5	4	0	52	97	136	161	187	228	259	279	308	360	7
	5<v≤10	8	0	82	130	162	182	205	230	252	275	299	360	9
	10<v≤15	8	0	117	172	192	211	235	259	273	285	306	360	8
	15<v≤20	20	0	170	192	213	238	250	261	273	285	297	360	11
	20<v≤25	38	0	196	208	216	228	238	245	257	269	286	360	13
	25<v	40	0	208	213	219	224	230	236	245	258	280	360	13
MAR	0<v≤5	2	0	21	96	127	161	180	212	239	265	307	360	7
	5<v≤10	6	0	59	115	145	175	204	235	261	279	309	360	7
	10<v≤15	10	0	148	188	206	219	236	255	268	286	307	360	7
	15<v≤20	15	0	144	193	211	224	237	251	262	278	297	360	7
	20<v	20	0	139	199	217	230	239	248	256	270	287	360	7
APR	0<v≤5	2	0	49	87	120	151	179	204	237	274	307	360	7
	5<v≤10	6	0	64	104	126	144	175	214	244	270	285	360	7
	10<v≤15	11	0	81	101	121	146	207	240	264	285	312	360	7
	15<v≤20	0	0	175	207	220	230	238	251	262	270	285	360	7
	20<v	0	0	210	220	230	240	252	261	267	275	292	360	7
MAY	0<v≤5	1	0	29	65	89	117	149	178	208	248	294	360	7
	5<v≤10	6	0	53	82	98	121	149	178	213	242	285	360	7
	10<v≤15	3	0	30	47	63	87	121	196	230	254	268	360	16
	15<v	1	0	14	34	56	221	229	236	246	259	281	360	12

* $a = \frac{d\phi}{dF_{\phi|v}}\Big|_{F_{\phi|v}=0}$

** $b = \frac{d\phi}{dF_{\phi|v}}\Big|_{F_{\phi|v}=1}$

Table 3-2. CONDITIONAL CUMULATIVE DISTRIBUTION OF WIND DIRECTION (DEGREES), GIVEN WIND SPEED AT 1 KM (m/sec), AT KSC GEOGRAPHICAL AREA, FOR SPLINE CURVE INTERPOLATION (Continued)

		CUMULATIVE FREQUENCY												
KSC	m/sec	a*	0	.10	.20	.30	.40	.50	.60	.70	.80	.90	1.00	b**
JUN	0<v≤5	2	0	56	90	120	148	167	197	220	248	285	360	10
	5<v≤10	3	0	62	90	115	141	172	188	217	241	265	360	16
	10<v≤15	6	0	93	155	183	202	216	224	232	242	257	360	19
	15<v	0	0	104	128	176	195	210	220	232	253	280	360	10
JUL	0<v≤5	11	0	84	126	149	172	185	202	221	241	264	360	16
	5<v≤10	17	0	117	141	160	179	201	220	237	250	267	360	16
	10<v≤15	17	0	107	147	164	205	220	236	246	260	274	360	16
	15<v	0	0	170	218	223	229	232	240	256	268	290	360	12
AUG	0<v≤5	3	0	38	83	119	138	156	177	202	240	277	360	10
	5<v≤10	10	0	83	115	133	158	185	210	227	242	263	360	15
	10<v≤15	3	0	33	154	191	210	225	237	245	254	272	360	14
	15<v	0	0	45	80	216	221	225	229	233	242	255	360	20
SEP	0<v≤5	6	0	45	72	96	116	137	169	206	245	301	360	7
	5<v≤10	5	0	40	63	81	94	110	135	168	217	255	360	16
	10<v≤15	7	0	44	55	75	87	99	135	176	207	251	360	19
	15<v≤20	7	0	26	43	64	94	146	197	210	240	262	360	16
	20<v≤25	3	0	43	52	59	73	111	209	215	225	245	360	16
	25<v≤30	0	0	31	83	122	138	162	227	235	260	287	360	11
	30<v	0	0	20	105	196	206	213	244	254	290	330	360	6
OCT	0<v≤5	2	0	18	48	73	98	133	176	223	271	312	360	6
	5<v≤10	2	0	20	43	58	71	90	122	199	258	301	360	8
	10<v≤15	1	0	11	30	55	67	79	92	114	203	270	360	14
	15<	0	0	6	16	29	67	90	219	242	262	290	360	6
NOV	0<v≤5	2	0	18	52	71	95	151	218	248	272	295	360	8
	5<v≤10	2	0	29	56	72	89	115	175	223	256	294	360	8
	10<v≤15	2	0	25	47	71	95	151	218	247	272	291	360	10
	15<v≤20	0	0	12	58	195	227	252	270	282	287	295	360	12
	20<v	0	0	34	56	214	236	246	259	268	281	304	360	8

Table 3-2. CONDITIONAL CUMULATIVE DISTRIBUTION OF WIND DIRECTION (DEGREES), GIVEN WIND SPEED AT 1 KM (m/sec), AT KSC GEOGRAPHICAL AREA, FOR SPLINE CURVE INTERPOLATION (Concluded)

KSC	m/sec	CUMULATIVE FREQUENCY												
		a*	0	.10	.20	.30	.40	.50	.60	.70	.80	.90	1.00	b**
DEC	$0<v\leq5$	2	0	29	94	122	148	185	218	247	285	313	360	6
	$5<v\leq10$	7	0	52	75	104	142	187	218	252	281	307	360	7
	$10<v\leq15$	4	0	46	84	153	189	213	240	260	285	306	360	9
	$15<v\leq20$	3	0	72	193	222	239	264	279	284	290	299	360	11
	$20<v$	0	0	100	156	237	253	270	285	300	315	332	360	2

* $a = \frac{d\phi}{dF_{\phi|v}}\Big|_{F_{\phi|v}=0}$

** $b = \frac{d\phi}{dF_{\phi|v}}\Big|_{F_{\phi|v}=1}$

Table 3-3. CONDITIONAL CUMULATIVE DISTRIBUTION OF WIND DIRECTION (DEGREES), GIVEN WIND SPEED AT 1 KM (m/sec) FOR SPLINE CURVE INTERPOLATION AT VAFB GEOGRAPHICAL AREA, FOR SPLINE CURVE INTERPOLATION

		CUMULATIVE FREQUENCY												
VAFB	m/sec	a*	0	.10	.20	.30	.40	.50	.60	.70	.80	.90	1.00	b**
JAN	0<v≤5	0	0	2	31	86	149	173	211	251	299	322	360	6
	5<v≤10	0	0	0	18	52	143	180	220	286	314	325	360	5
	10<v≤15	0	0	0	6	41	143	183	213	242	308	327	360	5
	15<v≤20	0	0	0	0	10	137	156	176	192	202	215	360	28
	20<v	0	0	120	160	179	191	202	211	236	260	285	360	26
FEB	0<v≤5	0	0	14	34	97	140	161	189	237	267	310	360	7
	5<v≤10	0	0	0	15	38	136	162	195	281	313	335	360	5
	10<v≤15	0	0	0	2	24	124	153	178	232	310	335	360	4
	15<	0	0	20	118	135	150	169	176	185	198	300	360	4
MAR	0<v≤5	0	0	24	82	131	157	184	216	254	307	330	360	5
	5<v≤10	0	0	0	6	22	85	192	275	308	322	335	360	4
	10<v≤15	0	0	3	17	135	164	209	291	310	330	345	360	4
	15<v	0	0	1	17	30	138	169	181	194	208	321	360	6
APR	0<v≤5	4	0	45	79	112	152	200	227	265	300	323	360	6
	5<v≤10	0	0	1	15	34	159	195	251	297	315	330	360	4
	10<v≤15	0	0	3	9	21	32	133	283	305	320	340	360	4
	15<v	0	0	0	0	0	10	80	136	170	325	350	360	4
MAY	0<v≤5	0	0	16	52	103	148	189	223	270	299	323	360	5
	5<v≤10	0	0	5	16	32	101	191	307	322	330	345	360	4
	10<v≤15	0	0	6	30	305	311	317	322	328	330	334	360	4
	15<v	0	0	0	0	0	0	0	40	305	330	345	360	2
JUN	0<v≤5	0	0	9	48	79	193	205	266	294	322	340	360	5
	5<v≤10	0	0	2	12	29	86	167	308	320	330	342	360	4
	10<v≤15	0	0	9	20	30	307	317	326	330	335	340	360	3
	15<v	0	0	0	0	0	30	308	314	320	326	332	360	6

* $a = \frac{d\phi}{dF_{\phi|v}}\Big|_{F_{\phi|v}=0}$

** $b = \frac{d\phi}{dF_{\phi|v}}\Big|_{F_{\phi|v}=1}$

Table 3-3. CONDITIONAL CUMULATIVE DISTRIBUTION OF WIND DIRECTION (DEGREES), GIVEN WIND SPEED AT 1 KM (m/sec) FOR SPLINE CURVE INTERPOLATION AT VAFB GEOGRAPHICAL AREA, FOR SPLINE CURVE INTERPOLATION (Concluded)

		CUMULATIVE FREQUENCY												
VAFB	m/sec	a*	0	.10	.20	.30	.40	.50	.60	.70	.80	.90	1.00	b**
JUL	$0<v\leq5$	0	0	10	38	76	140	176	213	259	305	331	360	5
	$5<v\leq10$	0	0	6	16	30	56	157	295	313	324	332	360	5
	$10<v$	0	0	0	10	310	315	320	325	330	335	340	360	4
AUG	$0<v\leq5$	0	0	15	47	115	164	196	255	284	306	330	360	5
	$5<v\leq10$	0	0	3	19	44	142	190	308	319	328	340	360	3
	$10<v\leq15$	0	0	0	0	131	149	170	315	325	335	345	360	1
	$15<v$	0	0	0	0	131	149	170	315	325	335	345	360	1
SEP	$0<v\leq5$	0	0	11	53	101	133	159	181	216	280	322	360	5
	$5<v\leq10$	0	0	6	26	60	124	146	161	281	330	345	360	3
	$10<v$	0	0	0	0	124	133	140	330	335	340	345	360	1
OCT	$0<v\leq5$	2	0	41	86	124	145	164	191	232	268	311	360	6
	$5<v\leq10$	0	0	0	6	14	27	47	148	200	287	330	360	3
	$10<v$	0	0	0	3	7	13	27	32	330	340	350	360	1
NOV	$0<v\leq5$	0	0	12	43	115	149	168	206	256	295	325	360	4
	$5<v\leq10$	0	0	5	28	115	136	155	179	217	266	316	360	6
	$10<v\leq15$	0	0	0	1	11	25	131	153	182	210	240	360	8
	$15<v$	0	0	9	31	142	161	172	178	185	194	270	360	2
DEC	$0<v\leq5$	7	0	61	97	140	162	183	214	269	293	320	360	5
	$5<v\leq10$	0	0	0	9	30	124	162	205	262	306	330	360	2
	$10<v\leq15$	0	0	0	13	58	146	212	277	312	328	340	360	3
	$15<v$	0	0	11	169	180	191	221	228	236	260	326	360	3

* $a = \frac{d\phi}{dF_{\phi|v}}\Big|_{F_{\phi|v}=0}$

** $b = \frac{d\phi}{dF_{\phi|v}}\Big|_{F_{\phi|v}=1}$

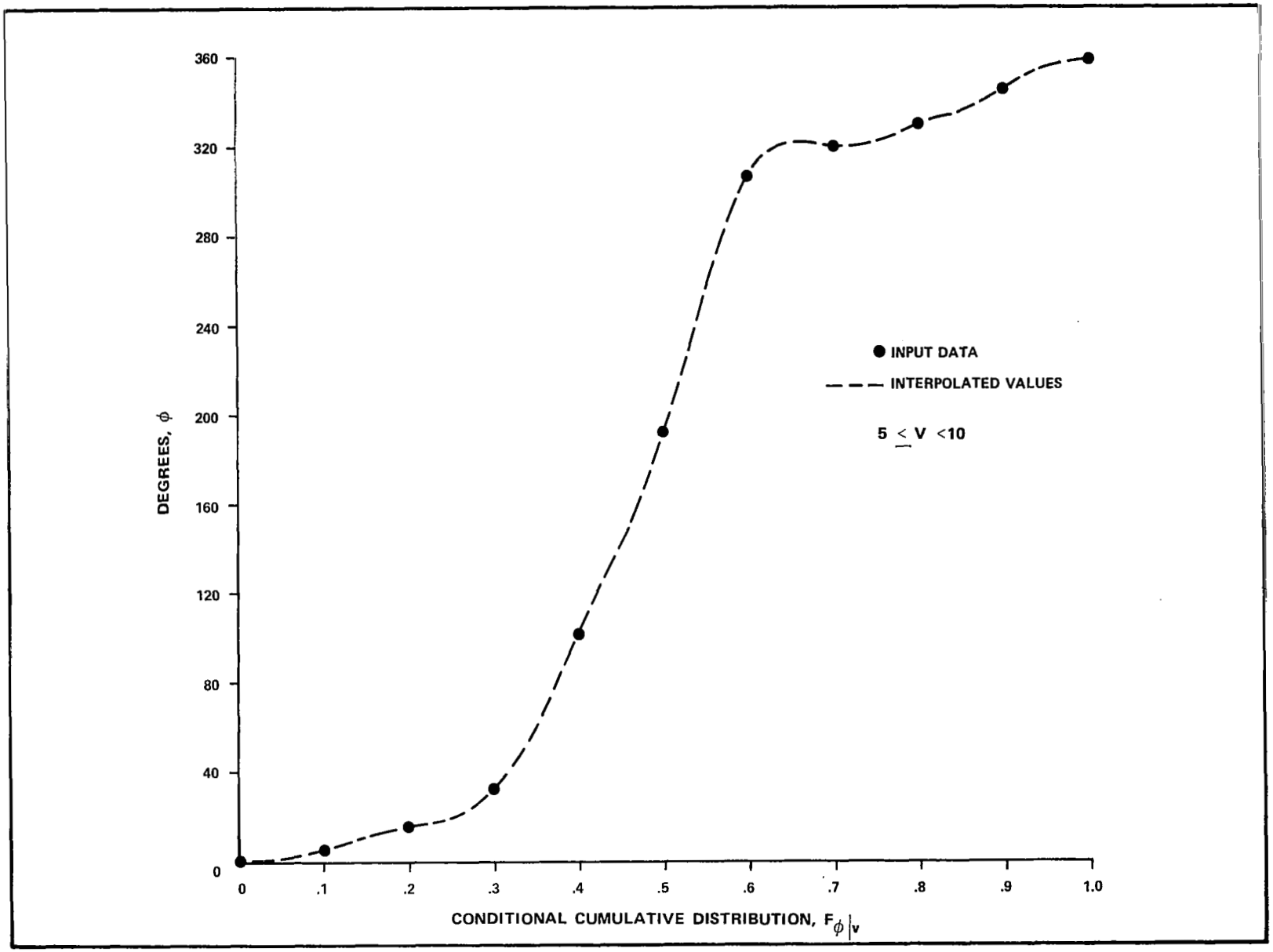

Figure 3-2. CONDITIONAL CUMULATIVE FREQUENCY, 1 KM WIND DIRECTION FOR GIVEN WIND SPEED, VAFB (1000 m) MAY

Section IV

LONG-CRESTED OCEAN WAVE MODEL

4.1 GENERAL

Long-crested wave heights η can be represented as a two-dimensional Fourier integral,

$$\eta(t,x) = \frac{1}{(2\pi)^2} \int_{-\infty}^{+\infty}\int \hat{\eta}(\sigma,k)\ e^{i(kx-\sigma t)}\ dk\ d\sigma \qquad (4.1.1)$$

where $\hat{\eta}$ is the Fourier spectrum, t is the time coordinate, and x is the distance coordinate taken in the direction of travel of the long-crested waves. The term k is the radian wave number and σ is the radian frequency. The inverse of Equation (4.1.1) is given by

$$\hat{\eta}(\sigma,k) = \int_{-\infty}^{+\infty}\int \eta(t,x)\ e^{-i(kx-\sigma t)}\ dx\ dt \quad . \qquad (4.1.2)$$

For deep water and shallow waves, the dispersion relationship (see Reference 7)

$$\sigma^2 = gk \qquad (4.1.3)$$

is commonly used, where g is the acceleration of gravity. This relationship relates the wave number to the frequency so that waves with small wave lengths will also have small cycle times. Since σ and k are directly related, then $\hat{\eta}(\sigma,k)=2\pi\ \hat{\eta}(\sigma)\ \delta(\sigma^2-k)$, where δ is the Dirac delta function. Then Equation 4.1.1 can be written as

$$\eta(t,x) = \frac{1}{2\pi} \int_{-\infty}^{+\infty} \hat{\eta}(\sigma)\ e^{i(kx-\sigma t)}\ d\sigma \qquad (4.1.4)$$

where k is now a function of σ as given by Equation (4.1.3). The above expression can also be written as

$$\eta(t,x) = \frac{1}{2\pi} \int_{-\infty}^{+\infty} \hat{\eta}_x(\sigma,x)\ e^{-i\sigma t} d\sigma \qquad (4.1.5)$$

where

$$\hat{\eta}_x = \hat{\eta}(\sigma)\ e^{ikx} \quad . \tag{4.1.6}$$

The inverse Fourier transform is then given by

$$\hat{\eta}_x(\sigma,x) = \int_{-\infty}^{+\infty} \eta(t,x)\ e^{i\sigma t}\ dt \quad . \tag{4.1.7}$$

Notice that it would have been possible to retain k-dependence instead of the σ-dependence. Then in Equation (4.1.4) the result would have been

$$\eta(t,x) = \frac{1}{2\pi} \int_{-\infty}^{+\infty} \hat{\eta}(k)\ e^{i(kx - \sigma t)}\ dk \tag{4.1.8}$$

which could have been written as

$$\eta(t,x) = \frac{1}{2\pi} \int_{-\infty}^{+\infty} \hat{\eta}_t\ e^{ikx}\ dk \quad . \tag{4.1.9}$$

Thus the present calculations can be carried out either in frequency or wave number space.

4.2 RELATIONSHIP OF FOURIER SPECTRUM TO POWER SPECTRUM

To relate the Fourier spectrum to the power spectrum, following Reference 5, for a specific value of x the following equation can be written

$$R_{\eta\eta}(\tau,x) = \lim_{T\to\infty} \frac{1}{T} \int_{-\frac{T}{2}}^{+\frac{T}{2}} \eta(t,x)\ \eta(t+\tau,x)\ dt \quad . \tag{4.2.1}$$

The Fourier transform (FT) of the above expression is

$$FT[R_{\eta\eta}(\tau,x)] = \lim_{T\to\infty} \frac{1}{T} \int_{-\frac{T}{2}}^{+\frac{T}{2}} \eta(t,x) \left[\int_{-\infty}^{+\infty} \eta(t+\tau,x)\ e^{i\sigma\tau}\ d\tau \right] dt \tag{4.2.2}$$

$$FT[R_{\eta\eta}(\tau,x)] = \lim_{T\to\infty} \frac{1}{T} \int_{-\frac{T}{2}}^{+\frac{T}{2}} \eta(t,x)\ \hat{\eta}_x(\sigma,x)\ e^{-i\sigma t}\ dt$$

$$= \lim_{T\to\infty} \frac{1}{T}\ \hat{\eta}_x^*(\sigma,x)\ \hat{\eta}_x(\sigma,x) \qquad (4.2.2)$$

Taking ensemble averages and using Equation (4.1.6), the power spectrum $S(\sigma)$ is given by

$$S(\sigma) = FT[R_{\eta\eta}] = FT[\langle R_{\eta\eta}\rangle] = \lim_{T\to\infty} \frac{1}{T} \langle \hat{\eta}^*(\sigma)\ \hat{\eta}(\sigma)\rangle \qquad (4.2.3)$$

where $R_{\eta\eta}$ is the autocorrelation,

$$R_{\eta\eta}(\tau) = \langle \eta(t)\ \eta(t+\tau)\rangle \qquad (4.2.4)$$

4.3 OCEAN WAVE SPECTRA FOR LONG-CRESTED WAVES

One ocean wave spectral distribution which is commonly used is the Pierson-Moskowitz model (Reference 6). This model applies to a "fully aroused sea." This is a sea in which all the Fourier components have been excited to the fully developed state by the wind stress. To attain these conditions, a wind must blow for a sufficiently long time over a sufficiently long fetch (distance over unobstructed water). The statistical characteristics of the "fully aroused sea" are considered constant.

The Pierson-Moskowitz spectrum can be written as

$$S(\sigma) = \pi\ \alpha\ \frac{g^2}{\sigma^5} \exp\left[-\beta \left(\frac{g}{v_o \sigma}\right)^4\right] \qquad (4.3.1)$$

where α and β are nondimensional universal constants

$$\alpha = 8.10 \times 10^{-3}$$

$$\beta = 0.74$$

and g is the acceleration of gravity given by

$$g = 9.8\ (m - sec^{-2})$$

v_o is the mean wind at the 19.5 m reference level in m-sec^{-1}, and σ is the radian frequency in radian-sec^{-1}. The units of the spectrum S are m^2/rad sec^{-1}. Since the autocorrelation is the inverse Fourier transform, (FT^{-1}), of the power spectrum,

$$R_{\eta\eta}(o) = FT^{-1}[S] = \frac{2}{2\pi} \int_o^\infty \frac{\pi\alpha g^2}{\sigma^5} \exp\left[-\beta\left(\frac{g}{v_o\sigma}\right)^4\right] d\sigma \qquad (4.3.2)$$

$$= \sigma_\eta^2 = \frac{\alpha v_o^4}{4\beta g^2}$$

4.4 NORMALIZATION OF THE VARIABLES

To simplify the power spectrum of Equation (4.3.1) the frequency is normalized to be

$$\omega = \sigma \frac{v_o}{g\beta^{1/4}} \qquad (4.4.1)$$

Since σt must be dimensionless, the dimensionless time must also be defined as

$$\tau = t\left(\frac{g\beta^{1/4}}{v_o}\right) \qquad (4.4.2)$$

so that

$$\omega\tau = \sigma t \quad . \qquad (4.4.3)$$

For this case the spectrum becomes

$$S(\sigma)d\sigma = S(\sigma)\left|\frac{d\sigma}{d\omega}\right| d\omega = S(\omega)d\omega \quad . \qquad (4.4.4)$$

Equation (4.4.4) can be written as

$$S(\omega)d\omega = \frac{\pi\alpha v_o^4}{g^2\beta} \frac{e^{-(\omega)^{-4}}}{\omega^5} d\omega = 4\pi \sigma_\eta^2 \frac{e^{-\omega^{-4}}}{\omega^5} d\omega \quad . \qquad (4.4.5)$$

From Equation (4.1.3)

$$k = \frac{\sigma^2}{g} = \frac{\omega^2 g\beta^{1/2}}{v_o^2} \qquad (4.4.6)$$

Thus, k can be normalized to be

$$\kappa = \frac{k v_o^2}{g\beta^{1/2}} = \omega^2 \quad . \tag{4.4.7}$$

Since kx must be dimensionless,

$$\chi = x \frac{g\beta^{1/2}}{v_o^2} \quad . \tag{4.4.8}$$

Then normalizing,

$$\rho = \frac{\eta}{\sigma_\eta} \quad . \tag{4.4.9}$$

Then from Equation (4.1.4)

$$\rho(\tau,x) = \frac{1}{2\pi} \int_{-\infty}^{+\infty} \hat{\rho}(\omega)\ e^{i(\kappa\chi - \omega\tau)}\ d\omega = \frac{1}{2\pi} \int_{-\infty}^{+\infty} \hat{\rho}_\chi\ e^{-i\omega\tau}\ d\omega \quad . \tag{4.4.10}$$

Then the autocorrelation and spectrum become

$$\frac{R_{\eta\eta}}{\sigma_\eta^2} = R_{\rho\rho} = \langle \rho(\tau)\ \rho(\tau + \Delta\tau) \rangle \tag{4.4.11}$$

and the power spectrum becomes

$$\frac{S(\omega)}{\sigma_\eta^2} = \psi(\omega) = \frac{4\pi e^{-\omega^{-4}}}{\omega^5} = \lim_{\tau\to\infty} \frac{1}{\tau} \langle \hat{\rho}^*(\omega)\ \hat{\rho}(\omega) \rangle \quad , \tag{4.4.12}$$

The power spectrum $\psi(\omega)$ is plotted on Figure 4-1. It can be seen that it is a narrow band spectrum with a maximum at ω=0.946.

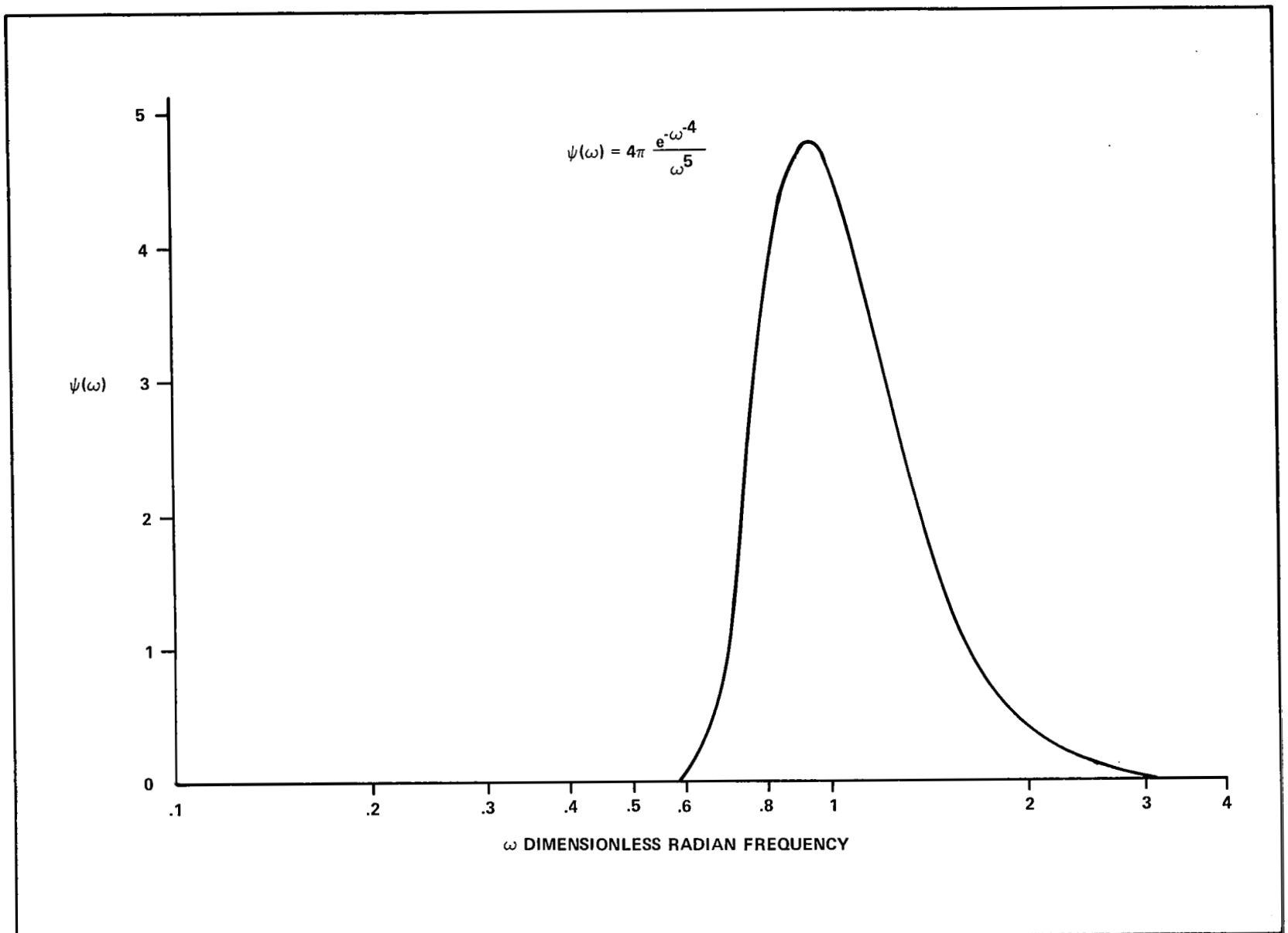

Figure 4-1. DIMENSIONLESS POWER SPECTRUM ψ

Section V

MONTE CARLO SIMULATION OF LONG-CRESTED WAVES

5.1 GENERAL

Two possible methods of simulating ocean waves will be presented in this section. One method uses a discrete Fourier series with randomly chosen coefficients and phase angles. The second method is a control system approach in which white noise is inputted through a linear system, and the output signal has the same statistical behavior as the simulated wave motion.

5.2 DISCRETE FOURIER SERIES SIMULATION

The dimensionless wave height over a period of dimensionless time τ_ρ for a given value of χ can be represented by a Fourier series (Reference 5)

$$\rho(\tau,\chi) = \sum_{n=-\frac{N}{2}}^{\frac{N}{2}} A_n(\omega,\chi)\ e^{(-i\omega_n\tau)} \tag{5.2.1}$$

where

$$\omega_n = \frac{2\pi n}{\tau_p} = n\Delta\omega \tag{5.2.2}$$

and

$$\Delta\omega = \frac{2\pi}{\tau_\rho}$$

and A_n is given by

$$A_n = \frac{1}{\tau_p} \int_{-\frac{\tau_p}{2}}^{+\frac{\tau_p}{2}} \rho\ e^{i\omega_n\tau}\ d\tau = \lim_{\tau_p\to\infty} \frac{1}{\tau_p}\ (\hat{\rho}_x(\omega_n) = \hat{\rho}(\omega_n)\ e^{(i\kappa_n\chi)}\ ; \tag{5.2.3}$$

then

$$A_n = \alpha_n\ e^{(i\kappa_n\chi)}\ \alpha_n = \lim_{\tau_p\to\infty}\ \frac{1}{\tau_p}\ (\hat{\rho}(\omega_n))\ . \tag{5.2.4}$$

Then

$$\rho = \sum_{n=-\frac{N}{2}}^{+\frac{N}{2}} \alpha_n \, e^{i(\kappa_n \chi - \omega_n \tau)} \quad . \tag{5.2.5}$$

This can be expanded to

$$\rho = \sum_{-\frac{N}{2}}^{+\frac{N}{2}} (\alpha_{R,n} + i\alpha_{I,n})(\cos(\kappa_n \chi - \omega_n \tau) + i \sin(\kappa_n \chi - \omega_n \tau)) \quad . \tag{5.2.6}$$

Since ρ is real, the imaginary term must be zero. As shown in Reference 5, this is because $\alpha_{R,n}$ is an even function and $\alpha_{I,n}$ is an odd function about $\omega_n = 0$. Then by expanding Equation (5.2.6)

$$\rho = \sum_{-\frac{N}{2}}^{+\frac{N}{2}} \alpha_{R,n} \cos(\kappa_n \chi - \omega_n \tau) - \alpha_{I,n} \sin(\kappa_n \chi - \omega_n \tau) \quad . \tag{5.2.7}$$

Since $\alpha_{R,n}$ is even and $\cos(\kappa_n \chi - \omega_n \tau)$ is even, the product is even. Similarl since $\alpha_{I,n}$ and $\sin(\kappa_n \chi - \omega_n \tau)$ are both odd functions then this product is an even function. Thus, the above can be written as

$$\rho = \alpha_{R,o} + 2 \sum_{n=1}^{N/2} [\alpha_{R,n} \cos(\kappa_n \chi - \omega_n \tau) - \alpha_{I,n} \sin(\kappa_n \chi - \omega_n \tau) . \tag{5.2.8}$$

It has been shown in Reference 5 that $\alpha_{R,n}$ and $\alpha_{I,n}$ are random Gaussian variabl where

$$f(\alpha_{R,n}, \alpha_{I,n}) = \frac{1}{2\pi \langle \alpha_n^2 \rangle} \, e^{-(\alpha_{R,n}^2 + \alpha_{I,n}^2)/2\langle \alpha_n^2 \rangle} \tag{5.2.9}$$

and

$$\langle \alpha_{R,n} \rangle = \langle \alpha_{I,n} \rangle = 0 \quad . \tag{5.2.10}$$

Furthermore,

$$\langle \alpha^2_{R,n} \rangle = \langle \alpha^2_{I,n} \rangle = \langle \alpha^2_n \rangle \quad . \tag{5.2.11}$$

From Equation (5.2.4), the following is obtained

$$\langle \alpha_n \alpha^*_n \rangle = \langle \alpha^2_{R,n} \rangle + \langle \alpha^2_{I,n} \rangle = 2\langle \alpha^2_n \rangle = \lim_{\tau_p \to \infty} \frac{1}{\tau_p^2} \langle \hat{\rho}(\omega_n)\, \hat{\rho}^*(\omega_n) \rangle \quad . \tag{5.2.12}$$

Then, from Equation (4.4.12)

$$2\langle \alpha^2_n \rangle = \lim_{\tau_p \to \infty} \frac{\psi(\omega_n)}{\tau_p} = \lim_{\tau_p \to \infty} \psi(\omega_n)\, \frac{\Delta\omega}{2\pi} \text{ when } n \neq 0 \quad . \tag{5.2.13}$$

However, when $\omega_n = 0$, $\langle \alpha^2_{I,n} \rangle = 0$, the above expression becomes

$$\langle \alpha^2_o \rangle = \lim_{\tau_p \to \infty} \frac{\psi(o)}{\tau_p} = \lim_{\tau_p \to \infty} \psi(o)\, \frac{\Delta\omega}{2\pi} \tag{5.2.14}$$

where $\psi(\omega_n)$ is given by Equation (4.4.12).

If the transformations

$$\alpha_{R,n} = \alpha_{\rho,n} \cos \varepsilon_n$$

$$\alpha_{I,n} = \alpha_{\rho,n} \sin \varepsilon_n \tag{5.2.15}$$

are used, then Equation (5.2.8) becomes

$$\rho = \alpha_{\rho,o} \cos \varepsilon_o + 2 \sum_{n=1}^{N/2} \alpha_{\rho,n} \cos(\kappa_n \chi - \omega_n \tau + \varepsilon_n) \tag{5.2.16}$$

where the joint distribution of $\alpha_{n\rho}$ and ε_n are obtained by transforming Equation (5.2.9) to obtain

$$f(\alpha_{\rho,n},\varepsilon_n)d\alpha_{\rho,n}d\varepsilon_n = f(\alpha_{\rho,n})d\alpha_{\rho,n}f(\varepsilon_n)\ d\varepsilon_n \tag{5.2.17}$$

which becomes

$$f(\alpha_{\rho,n})d\alpha_{\rho,n} = \frac{\alpha_{\rho,n}}{<\alpha_n^2>}\ e^{-\alpha_{\rho,n}^2/2<\alpha_n^2>}\ d\alpha_{\rho,n} \tag{5.2.18}$$

and

$$f(\varepsilon_n)d\varepsilon_n = \frac{1}{2\pi}\ d\varepsilon_n \quad . \tag{5.2.19}$$

Equations for randomly sampled values from Equation (5.2.18) and Equation (5.2.19), as shown in Reference 5, can be derived by using the uniform random number R in the following equations

$$\varepsilon_n = 2\pi\ R_{\varepsilon n} \tag{5.2.20}$$

$$\alpha_{\rho,n} = [2<\alpha_n^2>\ \ln\ (\frac{1}{R_{\alpha,n}})]^{1/2} \tag{5.2.21}$$

where $<\alpha_n^2>$ is given by Equations (5.2.13) and (5.2.14).

Equation (5.2.16) has been given in a number of References (for example, Reference 9) as a probablistic model for ocean waves, but it was not derived from basic equations as in the present case nor was it used as a simulation procedure. It had also been often assumed that $\alpha_{\rho,n}$ was constant rather than a random variable.

5.3 CONTROL SYSTEM SIMULATION

In the control system simulation, a random white noise signal, I, is inputted into a control system, H, designed so that the output $\rho(\chi,\tau)$ has the desired statistical behavior (Figure 5-1). Then using Equation (4.4.10)

$$\hat{\rho}_{\chi}(\omega,\chi) = \hat{\rho}(\omega)e^{i\kappa\chi} = H(\omega)\ I(\omega)e^{i\kappa\chi} \tag{5.3.1}$$

where

$$FT^{-1}[\hat{\rho}_{x}(\omega,\chi)] = \rho(\tau,\chi) \quad . \tag{5.3.2}$$

It can be seen that

$$<\hat{\rho}_{\chi}\ \hat{\rho}_{x}^{*}> = <\hat{\rho}(\omega)\ \hat{\rho}^{*}(\omega)> = H(\omega)\ H^{*}(\omega)\ <I(\omega)\ I^{*}(\omega)> \quad . \tag{5.3.3}$$

This can be written as

$$\psi(\omega) = H(\omega)\ H^{*}(\omega)\ \psi_{I}(\omega) \quad . \tag{5.3.4}$$

Since the input signal is white Gaussian noise with a unit spectrum, the wave spectrum is given by

$$\psi(\omega) = H(\omega)\ H^{*}(\omega) \quad . \tag{5.3.5}$$

In normalized form it becomes

$$\psi(\omega) = \frac{4\pi e^{-\omega^{-4}}}{\omega^{5}} = H(\omega)\ H^{*}(\omega) \quad . \tag{5.3.6}$$

The system function $H(\omega)$ which will transform the noise signal can be written in terms of a Fourier spectrum $A(\omega)$ and a phase angle $\phi(\omega)$

$$H(\omega) = A(\omega)\ e^{i\phi(\omega)} \tag{5.3.7}$$

Letting $\phi(\omega)$ be zero, obtain

$$H(\omega) = A(\omega) = (\psi(\omega))^{1/2} \quad . \tag{5.3.8}$$

Then the output signal can be expressed as

$$\hat{\rho}_{\chi} = [\psi(\omega)]^{1/2} \, e^{i\kappa\chi} \, I(\omega) \quad . \tag{5.3.9}$$

If the impulse response function h is

$$h(\tau;\chi) = FT^{-1} \, [(\psi(\omega))^{1/2} \, e^{i\kappa\chi}] \quad ; \tag{5.3.10}$$

then the wave signal is expressed as

$$\rho(\tau;\chi) = FT^{-1} \, (\hat{\rho}_{\chi}) = h(\tau;\chi) * I(\tau) \tag{5.3.11}$$

where * refers to the convolution integral

$$\rho(\tau;\chi) = \int_{-\infty}^{+\infty} h(\tau';\chi) \, I(\tau-\tau') \, d\tau' \quad . \tag{5.3.12}$$

Thus, by generating a noise signal and convolving it with the appropriate system function, a wave field in time and position can be generated. If a signal is desired for a point moving along the surface at some velocity v, then $\chi=v\tau$; and then equation (5.3.12) will give the wave signal in time for an observer moving with velocity v.

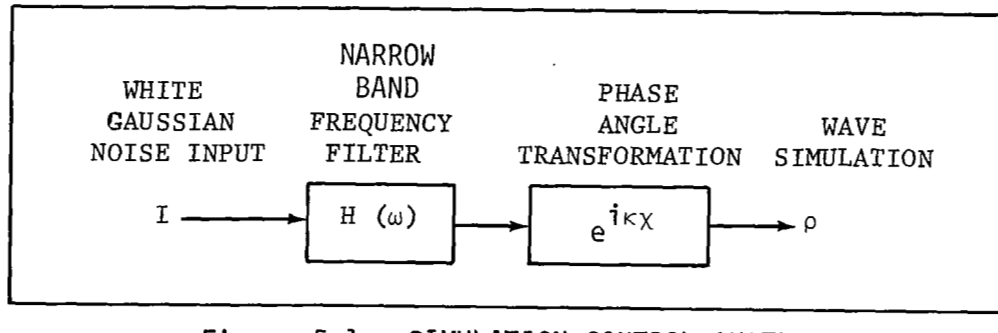

Figure 5-1. SIMULATION CONTROL SYSTEM

Section VI

WAVE CHARACTERISTICS

6.1 GENERAL

The quantities that describe the wave characteristics, specifically the probability distribution of wave heights, wave slopes, and velocities, are given in this section.

6.2 PROBABILITY DISTRIBUTION OF WAVE HEIGHTS

As discussed in References 7 and 10, the wave height has a Gaussian probability distribution given by

$$f(\rho) = \frac{1}{(2\pi\langle\rho^2\rangle)^{1/2}} \exp\left(-\frac{\rho^2}{2\langle\rho^2\rangle}\right) = N(\rho;\ 0,\ \langle\rho^2\rangle) \qquad (6.2.1)$$

where the $N(\rho;\langle\rho\rangle\ \langle\rho^2\rangle)$ refers to a normal distribution of ρ with a mean of $\langle\rho\rangle$ equal 0 and variance $\langle\rho^2\rangle$. The $\langle\rho^2\rangle$ is given by

$$\langle\rho^2\rangle = \frac{1}{2\pi}\int_{-\infty}^{+\infty} \psi(\omega)d\omega = M_{o,o} = 4\int_{o}^{\infty} \frac{e^{-\omega^{-4}}}{\omega^5}\, d\omega = 1 \quad . \qquad (6.2.2)$$

Thus, the normalized wave height has a Gaussian distribution with a mean of o and a variance of 1. The $M_{i,j}$ are moments of the spectrum and will be used more extensively later.

$$M_{i,j} = \frac{1}{2\pi}\int_{-\infty}^{+\infty} \omega^i k(\omega)^j\ \Psi(\omega)\ d\omega$$

Since very small waves will have very little effect on the Space Shuttle Solid Rocket Booster, it is worthwhile to truncate the spectrum, at some maximum frequency, ω_{max}. This will not change the mean value of the wave height distribution which will remain 0; however, the variance of the wave height will be reduced to $M^T_{o,o}$ which is the integral of the power spectrum up to ω_{max}

$$M^T_{o,o} = \frac{1}{\pi}\int_{o}^{\omega_{max}} \psi(\omega)d\omega = e^{-\frac{1}{\omega_m^4}} \qquad (6.2.3)$$

The distribution of wave height will now be given for the truncated spectrum case by

$$f_T(\rho) = N(\rho;o,M^T_{o,o}) \quad . \tag{6.2.4}$$

The values of $M^T_{o,o}$ for different values of ω_{max} are given in Table 6-1.

Table 6-1. VALUES OF MOMENTS OF POWER SPECTRUM TRUNCATED AT VARIOUS VALUES OF ω_{max}

ω_{max}	$M^T_{o,o}$	$M^T_{o,2}$	$M^T_{2,o}$	$M^T_{1,1}$
∞	1.0	∞	1.772	-3.625
10	0.9999	8.63	0.876	-3.226
3.16	0.99	4.04	0.787	-2.362
2.10	0.95	3.49	0.669	-1.740
1.75	0.90	1.775	0.572	-1.387

It is of interest to check the distribution of wave heights given by the Fourier series simulation procedure, Equation (5.2.11). The central limit theorem states that a random variable made up of a random sum will have a Gaussian distribution, permitting

$$f(\rho) = N(\rho;<\rho>,<\rho^2>) \quad . \tag{6.2.5}$$

It can be seen that by taking the ensemble average of Equation (5.2.16), where use is made of the fact that α and ε are statistically independent,

$$<\rho> = <\alpha_{\rho,o}><\cos\varepsilon_o> + 2\sum_{n=1}^{N/2} <\alpha_{\rho,n}> <\cos(\kappa_n\chi-\omega_n\theta+\varepsilon_n)> \quad . \tag{6.2.6}$$

Using Equation (5.2.19), obtain

$$\langle \cos \varepsilon_o \rangle = \int_o^{2\pi} \cos \varepsilon_o \frac{d\varepsilon_o}{2\pi} = 0 \tag{6.2.7}$$

$$\langle \cos(\kappa_n \chi - \omega_n \theta + \varepsilon_n) \rangle = \int_o^{2\pi} \cos(\kappa_n \chi - \omega_n \theta + \varepsilon_n) \frac{d\varepsilon_n}{2\pi} = 0 \tag{6.2.8}$$

so that $\langle \rho \rangle = 0$. For $\langle \rho^2 \rangle$, there is

$$\langle \rho^2 \rangle = \langle \alpha_{\rho,o}^2 \rangle \langle \cos^2 \varepsilon_o \rangle + 4 \sum_{n=1}^{N/2} \langle \alpha_{\rho,n}^2 \rangle \langle \cos^2(\kappa_n \chi - \omega_n \theta + \varepsilon_n) \rangle \ . \tag{6.2.9}$$

Cross-product terms are neglected since α and ε are statistically independent. Using Equation (5.2.18), obtain

$$\langle \alpha_{\rho,n}^2 \rangle = \int_o^{\infty} \alpha_{\rho,n}^2 \frac{\alpha_{\rho n}}{\langle \alpha_n^2 \rangle} \left(e^{-\alpha_{\rho,n}^2 / 2\langle \alpha_n^2 \rangle} \right) d\alpha_{\rho,n} = 2\langle \alpha_n^2 \rangle \ . \tag{6.2.10}$$

Similarly,

$$\langle \cos^2(\kappa_n \chi - \omega_n \theta + \varepsilon_n) \rangle = \frac{1}{2\pi} \int_o^{2\pi} \cos^2 (\kappa_n \chi - \omega_n \theta + \varepsilon_n) \, d\varepsilon_n = \frac{1}{2} \ . \tag{6.2.11}$$

Therefore,

$$\langle \rho^2 \rangle = \langle \alpha_o^2 \rangle + 4 \sum_{n=1}^{N/2} \langle \alpha_n^2 \rangle = \frac{1}{2\pi} \left[\psi(o) \Delta\omega + 2 \sum_{n=1}^{N/2} \psi(\omega_n) \Delta\omega \right] \tag{6.2.12}$$

$$= \frac{1}{2\pi} \int_{-\infty}^{\infty} \psi(\omega) d\omega = M_{o,o} \ .$$

This gives the same result obtained in Equation (6.2.1). It is also of interest to check the control system simulation to see if it gives the appropriate distribution of wave heights. From Equation (5.3.1)

$$\rho(\tau,\chi) = \frac{1}{2\pi} \int_{-\infty}^{+\infty} e^{i\kappa\chi} H(\omega) I(\omega) e^{-i\omega\tau} d\omega \quad . \tag{6.2.13}$$

Inputting a white noise Gaussian process into a linear system gives a Gaussian output so that

$$f(\rho) = N(\rho; <\rho>, <\rho^2>) \tag{6.2.14}$$

where

$$<\rho> = FT^{-1} [e^{i\kappa\chi} H(\omega) <I(\omega)>] = 0 \tag{6.2.15}$$

and $<\rho^2> = \frac{1}{2\pi} \int_{-\infty}^{+\infty} \psi(\omega)d\omega = \frac{1}{2\pi} \int_{-\infty}^{+\infty} H(\omega) H^*(\omega)d\omega = M_{o,o}$; (6.2.16)

the result agrees with the previous result.

6.3 PROBABILITY DISTRIBUTION OF WAVE SLOPES

The normalized wave slope is given by

$$\frac{d\rho}{d\chi} = \rho_\chi = \frac{1}{2\pi} \int_{-\infty}^{+\infty} \hat{\rho}(\omega) (i\kappa) e^{i(\kappa\chi-\omega\tau)} d\omega \quad . \tag{6.3.1}$$

As pointed out previously, a Gaussian random signal passing through a linear system will remain Gaussian; therefore,

$$f(\rho_\chi) = N(\rho_\chi; <\rho_\chi>, <\rho_\chi^2>) \quad . \tag{6.3.2}$$

From Equation (6.2.13) it can be seen that

$$\rho_\chi = \frac{1}{2\pi} \int_{-\infty}^{+\infty} (i\kappa) e^{i\kappa\chi} H(\omega) I(\omega) e^{-i\omega\tau} d\omega \quad . \tag{6.3.3}$$

Then $\langle \rho_\chi \rangle = 0$ as before, and the spectrum is given by

$$\langle \hat{\rho}_\chi \hat{\rho}_\chi^* \rangle = \kappa^2 H(\omega) H^*(\omega) = \kappa^2 \psi(\omega) \quad . \tag{6.3.4}$$

Thus,

$$\langle \rho_\chi^2 \rangle = \frac{1}{2\pi} \int_{-\infty}^{+\infty} \kappa^2 \psi(\omega) d\omega = M_{o,2} \tag{6.3.5}$$

where, using the dispersion relationship (Equation (4.4.7)),

$$M_{o,2} = 4 \int_o^\infty \omega^4 \frac{e^{-\omega^{-4}}}{\omega^5} \, d\omega \quad .$$

Letting $y = \frac{1}{\omega^4}$, the above becomes

$$M_{o,2} = \int_o^\infty \frac{e^{-y}}{y} \, dy \quad .$$

As before, interest lies in the slopes due to the larger waves, and the advantage of removing the effects of the smaller waves which will not affect the Space Shuttle Solid Rocket Booster. By retaining the lower frequency fraction of the spectrum and letting the spectrum be zero for values greater than ω_{max}, the slope distribution is now given by

$$f_T(\rho_\chi) = N(\rho_\chi; 0, M_{o,2}^T)$$

where

$$M_{o,2}^T = \frac{1}{\pi} \int_o^{\omega_{max}} \kappa^2 \psi(\omega) d\omega = \int_{\frac{1}{\omega_{max}^4}}^\infty \frac{e^{-y}}{y} dy = EI\left(\frac{1}{\omega_{max}^4}\right)$$

and EI refers to the exponential integral. This is evaluated for several truncations, and the values are shown in Table 6-1.

6.4 FREQUENCY DISTRIBUTION OF WAVE VERTICAL VELOCITIES

The normalized vertical wave velocity is given by

$$\frac{d\rho}{d\tau} = \dot{\rho}_\tau = \frac{1}{2\pi} \int_{-\infty}^{+\infty} \hat{\rho}(\omega)(-i\omega)\, e^{i(\kappa\chi - \omega\tau)}\, d\omega \,. \tag{6.4.1}$$

As previously discussed, ρ_τ will have a Gaussian distribution

$$f(\rho_\tau) = N(\rho_\tau; 0, M_{2,o}) \tag{6.4.2}$$

where the variance is given by

$$M_{2,o} = \langle \rho_\tau^2 \rangle = \frac{1}{2\pi} \int_{-\infty}^{+\infty} \omega^2\, \psi(\omega) d\omega = 4 \int_o^\infty \omega^2\, \frac{e^{-\omega^{-4}}}{\omega^5}\, d\omega$$

$$= \sqrt{\pi} = 1.772 \,. \tag{6.4.3}$$

Primary interest is in the vertical velocities of the large waves. If the higher frequencies are removed from the spectrum, the result will be a truncated wave vertical velocity distribution

$$f_T(\rho_\tau) = N(\rho_\tau; o, M_{2,o}^T) \tag{6.4.4}$$

where

$$M_{2,o}^T = \frac{1}{\pi} \int_o^{\omega_{max}} \omega^2 \psi(\omega) d\omega = 4 \int_o^{\omega_{max}} \frac{e^{-\omega^{-4}}}{\omega^3}\, d\omega$$

$$= \int_{\frac{1}{\omega_{max}^2}}^{\infty} e^{-y^2}\, dy = \frac{\sqrt{\pi}}{2} \operatorname{erfc}\left(\frac{1}{\omega_{max}^2}\right) \tag{6.4.5}$$

and erfc refers to the complementary error function integral. These results are given in Table 6-1 for various values of ω_{max}.

6.5 FREQUENCY DISTRIBUTION OF HORIZONTAL WAVE VELOCITY

Consider a point on the wave surface at some height η, time τ, and position χ. At some later incremental time the wave surface will move to a new point $\chi+\Delta\chi$ at time $\tau+\Delta\tau$ but at the same height η.

$$d\rho = \left(\frac{\partial\rho}{\partial\chi}\right)d\chi + \left(\frac{\partial\rho}{\partial\tau}\right)d\tau = 0 \quad . \tag{6.5.1}$$

The normalized horizontal velocity is given by

$$\chi_\tau = \frac{d\chi}{d\tau} = -\left(\frac{\frac{\partial\rho}{\partial\tau}}{\frac{\partial\rho}{\partial\chi}}\right) = -\frac{\rho_\tau}{\rho_\chi} \quad . \tag{6.5.2}$$

The joint Gaussian distribution of ρ_τ and ρ_χ can be expressed as

$$f(\rho_\tau,\rho_\chi) = \frac{1}{2\pi\Delta^{1/2}} \exp\left[-(M_{2,o}\,\rho_\chi^2 - 2\,M_{1,1}\,\rho_\chi\rho_\tau + M_{o,2}\,\rho_\tau^2)/2\Delta\right] \tag{6.5.3}$$

where

$$\Delta = M_{2,o}\,M_{o,2} - M_{1,1}^{\,2} \quad .$$

This joint Gaussian can be transformed to the new variable

$$\chi_\tau = -\frac{\rho_\tau}{\rho_\chi} \; ; \; y = \rho_\tau$$

to give

$$f(\chi_\tau,y) = \frac{1}{2\pi\Delta^{1/2}} \,|J|\, \exp\left[-y^2\left(\frac{M_{2,o}}{\chi_\tau^2} + \frac{2M_{1,1}}{\chi_\tau} + M_{o,2}\right)/2\Delta\right] \tag{6.5.4}$$

where the Jacobian is given by

$$|J| = \left|\frac{y}{\chi_\tau^2}\right| \quad .$$

This can be integrated over the y variable from $-\infty$ to $+\infty$ to give

$$f(\chi_\tau) = \frac{\Delta^{1/2}}{\pi} \frac{1}{M_{o,2}\,\chi_\tau^2 + 2\,M_{1,1}\,\chi_\tau + M_{2,o}} \quad . \tag{6.5.5}$$

This gives the distribution of the horizontal velocity.

It can be found that the maximum or mode of the distribution is given by

$$\chi_\tau^M = -\frac{M_{1,1}}{M_{o,2}} \quad . \tag{6.5.6}$$

Then

$$f(\chi_\tau) = \frac{\Delta^{1/2}}{\pi M_{o2}\,[\chi_\tau^2 - 2\chi_\tau\,\chi_\tau^M + \frac{M_{2,o}}{M_{o,2}}]} \tag{6.5.7}$$

$$= \frac{\Delta^{1/2}}{\pi\,M_{o,2}\left[(\chi_\tau - \chi_\tau^M)^2 - \frac{M_{1,1}^2}{M_{o,2}^2} + \frac{M_{o,2}M_{2,o}}{M_{o,2}^2}\right]}$$

which can be expressed as

$$f(\chi_\tau) = \frac{\Delta^{1/2}}{\pi M_{o,2}\left[(\chi_\tau - \chi_\tau^M)^2 + \frac{\Delta}{M_{o,2}^2}\right]} \quad . \tag{6.5.8}$$

This is a Cauchy distribution with a maximum at $\chi_\tau^M = -M_{1,1}/M_{o,2}$, and the distribution is symmetrical at χ_τ^M.

For purely progressive waves, since κ and ω must be of opposite signs, and remembering that $\kappa = \omega^2$,

$$M_{1,1} = -\frac{1}{\pi}\int_0^\infty \kappa\omega\psi(\omega)d\omega = -4\int_0^\infty \omega^3 \frac{e^{-\omega^{-4}}}{\omega^5} d\omega \quad . \tag{6.5.9}$$

This can be rewritten with $y = \frac{1}{\omega^4}$ as

$$M_{1,1} = -\int_0^\infty \frac{e^{-y}}{y^{3/4}} dy = -\Gamma(\tfrac{1}{4}) = -3.625 \tag{6.5.10}$$

where Γ represents the gamma integral.

As before, the interest is in the horizontal velocity of the larger waves. The spectrum will extend only to ω_{max} and the integral becomes the incomplete Gamma function

$$M^T_{1,1} = -\int_{y=\frac{1}{\omega_{max}^4}}^\infty \frac{e^{-y}}{y^{3/4}} dy = -\Gamma(\tfrac{1}{4}, \tfrac{1}{\omega_{max}^4}) \quad . \tag{6.5.11}$$

6.6 VELOCITY FIELD BELOW THE WATER SURFACE

As discussed in Reference 9, the horizontal and vertical velocity below the surface can be related to the motion on the surface by using the referenced "Long-Crested Gaussian Linear Eularian Model of Random Waves." If Equation 5.2.16 is used for the surface wave model, then the horizontal velocity u and the vertical velocity w at height z is given by

$$u = \alpha_{\rho,o}\cos\varepsilon_o + 2\sum_{n=1}^{N/2}\alpha_{\rho,n}(\exp(-\kappa_n z))\cos(\kappa_n\chi - \omega_n\theta + \varepsilon_n) \tag{6.5.12}$$

and

$$w = \alpha_{\rho,o}\cos\varepsilon_o + 2\sum_{n=1}^{N/2}\alpha_{\rho,n}(\exp(-\kappa_n z))\sin(\kappa_n\chi - \omega_n\theta + \varepsilon_n) \tag{6.5.13}$$

where Z gives the depth below the surface.

Section VII

CONCLUSIONS

This report presents the pertinent features of a study of the effect on the Space Shuttle Solid Rocket Booster of oceanic impact and the subsequent recovery. Data on the statistical distribution of ocean currents in the planned splashdown areas are given in a form suitable for use in simulation studies. This is because spline fitting can be used for interpolation in the random sampling procedure of the simulation.

The influence of 1-kilometer winds on wave behavior is also discussed. The ocean model based on random function analysis and assumed long-crested waves is developed. Using the Pierson-Moskowitz power spectrum distribution of wave height, wave slope and wave velocity are given. The velocity of the fluid below the surface based on the linear Eularian model is also shown.

Two simulation procedures are developed, but no extensive numerical calculations are presented. Such numerical calculations for the simulation models as well as extension of the results of the long-crested wave model are currently being done for the case where waves can move in all directions.

Section VIII

REFERENCES

1. Shreider, Y. A., "The Monte Carlo Method," Pergamon Press, Long Island City, New York, 1966.

2. UNIVAC Large Scale Systems Math Pack, UP4051 Rev. 2, UNIVAC, 1970.

3. "Environmental Conditions within Specified Geographical Regions Offshore East and West Coasts of the United States and in the Gulf of Mexico," National Data Buoy Center, NOAA, August 13, 1970.

4. Brown, S. C., "Cape Kennedy Wind Component Statistics Monthly and Annual Reference Periods for all Flight Azimuths from 0 to 70 km Altitude," NASA TM 53956, October 1969.

5. Perlmutter, M., "Randomly Fluctuating Flow in a Channel Due to Randomly Fluctuating Pressure Gradients," NASA TN-D6213-1971.

6. Daniels, G. E., Editor "Terrestrial Environment (Climate) Criteria Guidelines for Use in Aerospace Vehicle Development," 1973 Revision, NASA TMX-64757, July 1973.

7. Kinsman, B., "Wind Waves," Prentice-Hall, Inc., Englewood Cliffs, N. J., 1965.

8. Longuet-Higgens, M. S., "Statistical Properties of Moving Wave Form," Cambridge Phil. Soc., Vol. 52, Pg. 2, 1956.

9. Neumann, G. and Pierson, W. J., Jr., "Principals of Physical Oceanography," Prentice-Hall, Inc., Englewood Cliffs, N. J., 1966.

10. Phillips, O. M., "The Dynamics of the Upper Ocean," Cambridge Press, 32E 57ST, New York, N. Y., 1966.

11. Longuet-Higgins, M. S., "The Statistical Geometry of Random Surfaces," Proceedings of Symposia in Applied Math, Vol. 13, AMS, Providence, R. I., 1962.

12. Papoulis, A., "Probability Random Variables and Stochastic Processes," McGraw Hill Book Company, New York, N. Y., 1965.